ACS Sustainable Chemistry & Engineering

pubs.acs.org/journal/ascecg

Research Article

Synthesis of Biobased Novolac Phenol–Formaldehyde Wood Adhesives from Biorefinery-Derived Lignocellulosic Biomass

Archana Bansode, Mehul Barde, Osei Asafu-Adjaye, Vivek Patil, John Hinkle, Brian K. Via, Sushil Adhikari, Andrew J. Adamczyk, Ramsis Farag, Thomas Elder, Nicole Labbé, and Maria L. Auad*

Cite This: *ACS Sustainable Chem. Eng.* 2021, 9, 10990–11002

Read Online

ACCESS | Metrics & More | Article Recommendations | Supporting Information

ABSTRACT: Lignocellulosic biomass is a sustainable alternative to petroleum-derived chemicals to develop biobased wood adhesives, which motivates integrated biorefineries to effectively convert biomass feedstock into desirable chemicals. Herein, lignin recovered from kraft biorefinery (L-KB) and two bio-oils, prepared from laboratory-scale solvent liquefaction of lignin (BO-SL/L) and fast pyrolysis of pinewood (BO-FP/PW), respectively, have been used to substitute 50% (w/w) of phenol in a novolac phenol–formaldehyde (NPF) resin system. The molecular structures of the L-KB, BO-SL/L, and BO-FP/PW were characterized via FTIR, $^{13}C-^{1}H$ HSQC 2D-NMR, GCMS, and carbohydrate analysis. Characterization results revealed the presence of functional moieties derived from lignin and polysaccharides. Further, the obtained resin adhesive structures were examined by FTIR and ^{1}H NMR spectroscopy, which confirmed the formation of methylene bridges during the resin preparation. Subsequently, to understand the curing behavior of each of the NPF resins with hexamethylenetetramine (HMTA) curing agent, DSC analysis was performed, which helped to optimize the bonding process. The resulting bonding strength of each resin adhesive, measured by gluing two pieces of wood, indicated significantly different adhesion ability due to structural differences, which was analyzed by two-way ANOVA, followed by Tukey's post hoc test. The 50-NPF-L-KB adhesive demonstrated a tensile shear strength of 3.46 ± 0.55 MPa, higher than the values of other tested adhesives. This indicates that the lignin derived from kraft biorefinery is a potential substitute for phenol in the NPF resin system for use in wood adhesive applications.

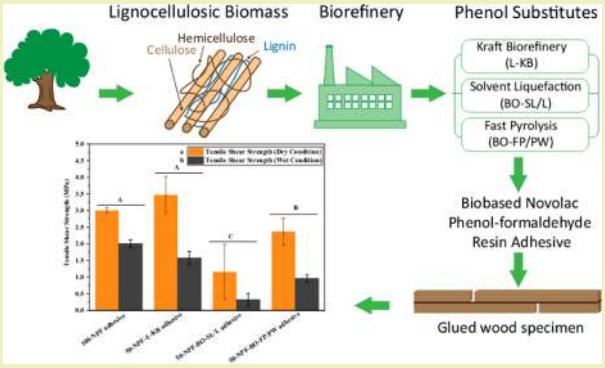

KEYWORDS: *kraft lignin, solvent liquefaction, fast pyrolysis, bio-oil, structural characterization, polymerization, curing, adhesion strength*

INTRODUCTION

The large-scale production and use of adhesives to develop wood-based composites have been rapidly expanding over the years.[1] These adhesives are mainly produced from petroleum-derived monomers. However, the utilization of these monomers and their corresponding materials are growing concerns owing to environmental pollution and future shortages of energy supplies.[2] In this context, integrated biorefineries have been proposed at the industrial and laboratory scale to facilitate the production of sustainable chemicals and fuels through renewable feedstocks.[3] Lignocellulose is one of the most desirable renewable feedstocks, composed of three biopolymers: cellulose, hemicellulose, and lignin. These biopolymers are generally derived from residues of industrial (e.g., black liquor), agricultural (e.g., wheat straw), and forestry waste (e.g., sawdust) as well as energy crops.[4,5]

In the quest to utilize lignocellulosic biomass (LCBM), kraft biorefinery represents a cost-effective and zero-waste strategy.[6] Kraft is a pulping process of transforming wood into wood pulp; during this operation, cellulose is separated by dissolving lignin from lignocellulosic biomass in an alkaline medium (NaOH and Na_2S). At the end of the process, a high solids concentration called black liquor is generated as a byproduct, which contains a significant lignin concentration in addition to hemicellulose and other chemicals.[7] In this line, several technically feasible processes have been pioneered to extract lignin from black liquor by acidification. For instance, Westvaco (now called Ingevity) is the most established technology for kraft lignin recovery at a commercial scale, enabling high-purity lignin (e.g., Indulin-Westvaco's trade name) production.[8,9] This lignin is a highly functionalized biomacromolecule that contains various reactive groups such as acidic, aliphatic, and aromatic hydroxyl, whose relative chemistry is applicable in the synthesis of biobased materials.[10]

Received: March 19, 2021
Revised: July 29, 2021
Published: August 10, 2021

A thermochemical conversion process is another explicitly endorsed biorefinery strategy to convert biomass to energy. Intensive reaction conditions are employed to break the bonds of organic matter and provide a wide range of chemical compounds that can be used to produce biobased materials.[11] This includes technologies such as pyrolysis, liquefaction, gasification, and combustion. Liquefaction and pyrolysis are considered high-efficiency conversion technologies which produce bio-oil (a mixture of oxygenated compounds) as a predominant product with a high energy density compared to solid biomass.[12] Liquefaction is performed in an aqueous environment (hydrothermal liquefaction) or organic solvents (solvent liquefaction).[13] Usually, solvent liquefaction can be performed at modest temperatures (105−400 °C) and elevated pressures (2−20 MPa) in the presence of a suitable solvent.[14] The performance of the liquefaction process depends on the selection of a suitable solvent. In this case, alcohols are proved to be a suitable solvent, as they suppress side reactions by providing hydrogen sources during the reaction.[15] In this regard, research work in the literature reported that solvent liquefaction of lignin, using alcohol as a solvent, showed a higher conversion efficiency. This is important in the case of lignin, as there can be a chance of getting a high amount of solid fraction recoupling of phenolic compounds.[16]

As mentioned above, pyrolysis is a robust thermochemical process of materializing biomass into valuable and flexible bio-liquids, which is commonly performed at moderate temperatures (450−600 °C) under oxygen-free conditions.[17] According to the pyrolysis process parameters, two main pyrolysis processes are listed: slow pyrolysis (conventional pyrolysis) and fast pyrolysis. Fast pyrolysis is a productive method in which the biomass is rapidly heated to high temperatures for a very short residence time, leading to the low investment cost and high-yield bio-oil.[18] The obtained fast pyrolysis liquid fraction shows phase-separated bio-oil. The lower phase is classified as organic and mainly originates from pyrolytic lignin, while the upper phase is more of aqueous fractions.[19] The main reason for phase separation is excess water, which resulted in a byproduct of condensation and esterification reactions at elevated temperatures.

Interestingly, the organic phase of bio-oil can be practically useful in producing aromatic chemicals due to the high concentration of phenolic compounds. However, the chemical composition of bio-oil depends on the feedstock used during fast pyrolysis.[20,21] For the explained reasons, these noteworthy biorefinery materials (kraft recovery lignin and thermochemical conversion bio-oils) hold the potential to replace the petroleum-based monomers in conventional adhesive production.

Phenol−formaldehyde (PF) resin is a widely used adhesive in various wood industries and synthesized via condensation polymerization of phenol and formaldehyde using either acid (oxalic acid or hydrochloric acid) or base (sodium hydroxide) catalyst to produce novolac or resole PF resin, respectively.[22] However, novolac PF resins are produced with an excess of phenol, classified as a hazardous substance derived from petroleum sources.[23] Therefore, the substitution of phenol with biobased phenolic structures becomes an alternative sustainable strategy to produce biobased novolac PF wood adhesives. Several studies have reported biobased resole PF resins from lignocellulosic biomass (LCBM) for wood adhesive application.[24−27] However, limited literature has reported the substitution of phenol by LCBM in novolac PF resin preparation.[28,29] A wide variety of lignocellulosic biomass has been proposed in the literature for producing biobased wood adhesives. Among these, the softwood and grass-containing LCBM is considered as a prime choice for PF adhesive, as it possesses more guaiacyl (G) and *p*-hydroxyphenyl (H) units in its structure, which can react with formaldehyde in PF resin synthesis.[24]

In this study, we have selected phenolic structures from three different biorefineries: lignin from kraft biorefinery (L-KB), bio-oil produced from solvent liquefaction of industrial lignin (BO-SL/L), and bio-oil obtained from fast pyrolysis of pinewood (BO-FP/PW) for the synthesis of NPF resin adhesive. The first two sources are lignin powder and bio-oil from lignin, so they are lignin-based. In contrast, the BO-FP/PW is obtained from the organic phase of bio-oil, mainly pyrolytic lignin, as demonstrated by previous work from this group.[30] In addition, kraft lignin (L-KB) and the BO-FP/PW are produced from softwood sources. All of the biobased sources were characterized and compared in the first part of this work. We then used these phenolic sources to substitute 50% (w/w) of phenol in the Novolac phenol−formaldehyde (NPF) resin system. Finally, these biobased NPF resins were compared to 100-NPF resin (lab-made novolac PF) as a reference. The adhesion properties were determined using tensile shear strength analysis on the wood sample under dry and wet conditions using the proper standard method. The performance of adhesives was discussed with the help of two-way ANOVA, followed by Tukey's post hoc test.

EXPERIMENTAL SECTION

Materials. The kraft lignin (Indulin AT) used in this work was generously provided by Ingevity Corporation, South Carolina. Deuterated dimethyl sulfoxide (DMSO-d_6, with TMS 0.1 vol % deuteration degree min 99.9%), pyridine (>99%), acetic anhydride (≥97.0%), tetrahydrofuran (THF, 99.0%), glucose, sulfuric acid (70%), phenol (99%), formalin solution (37% formaldehyde in water with 10−15% methanol as stabilizer), hexamethylenetetramine (HMTA, >99%), and acetone (99.5%) were purchased from VWR International. Oxalic acid (anhydrous crystal, 98.0%) was supplied by Spectrum Chemical Mfg. Corp. Southern yellow pine (*Pinus* spp.) wood was used in the adhesion properties studies. The solvent liquefaction bio-oil (BO-SL/L) and fast pyrolysis (BO-FP/PW) were obtained from lignin and pinewood, respectively. The relevant biorefinery processes were performed in our Biosystems Engineering Laboratory, Auburn University, and the Center for Renewable Carbon Laboratory, University of Tennessee, as described in the following methodology.

Solvent Liquefaction Methodology. The lignin used for solvent liquefaction was provided by Renmatix Incorporation. The lignin was made using a proprietary supercritical water extraction technology. The details of feed biomass were not provided by the supplier. A 1.8 L capacity high-pressure Parrr 4680 reactor was used for solvent liquefaction to produce bio-oil from lignin. Briefly, 100 g of lignin thoroughly mixed with 500 mL of ethanol (reagent grade, 95%, VWR International) was loaded into the reactor vessel.[31] The reactor was then pressurized and depressurized with 300 psi nitrogen (ultrahigh purity, 99.999%) thrice and then heated to 250 °C with stirring at 500 rpm. The maximum pressure attained by the reactor was ∼1400 psi at 250 °C. The reactor was then washed with ethyl acetate (VWR International) to remove any product stuck on the impeller, and this mixture was added to the product.[32] The product mixture was filtered with Whatman filter paper (no. 42) to separate the char. The filtrate was subjected to rotary evaporation at 40 °C under vacuum to remove ethyl acetate and ethanol. The resulting bio-oil was removed from the round-bottom flask by mixing it with

https://doi.org/10.1021/acssuschemeng.1c01916
ACS Sustainable Chem. Eng. 2021, 9, 10990−11002

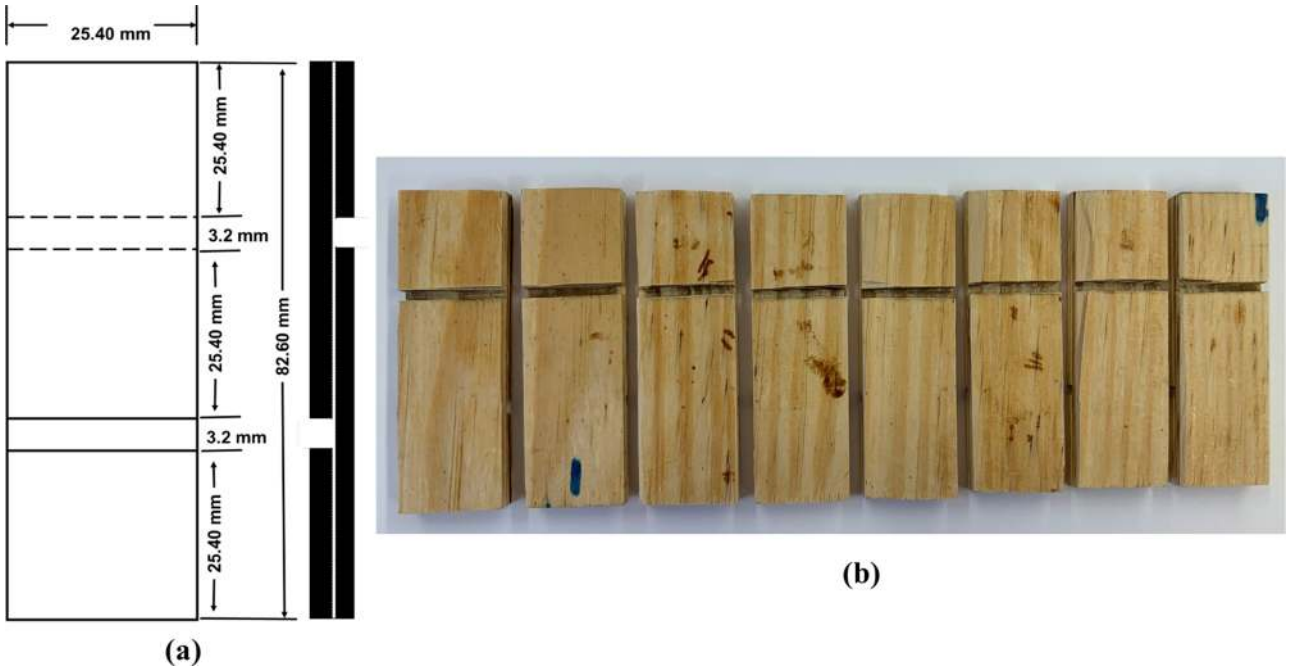

Figure 1. (a) Schematic illustration of the dimension of the wood specimen (ASTM D906-98 2017).[41] (b) Wood specimens glued with NPF resin adhesives.

dichloromethane (≥99.5%, VWR International) and then keeping it under vacuum at room temperature for 24 h. The bio-oil was obtained in ∼55 wt % yields (based on the initial dry mass of lignin). The exact process was repeated twice, and the bio-oil was combined.

Fast Pyrolysis Methodology. A semi-pilot scaled auger reactor was used for the fast pyrolysis experiment, and the details about reactor design are explained previously.[33] For the experiment, pinewood biomass with particles less than 4 mm in size was fed into a pyrolyzer reactor at a rate of 7.3 kg/h. The pyrolysis reaction occurred at 500 °C under oxygen-free conditions by continuously passing N_2 at a flow rate of 50 L/min. After condensation of pyrolysis vapors in the quench system, the liquid products were allowed to settle down to separate the organic phase of bio-oil from the aqueous phase. The related properties of bio-oil are reported in previously published articles from our research group.[30,34]

Characterization of L-KB, BO-SL/L, and BO-FP/PW. *FTIR Spectroscopy.* FTIR measurements were performed using a Thermo Scientific Nicolet 6700 FTIR instrument equipped with attenuated total reflection (ATR). Each spectrum was collected with 64 scans in the wavenumber range of 4000−400 cm^{-1} at a resolution of 4 cm^{-1}. Background spectra were recorded before every sampling. The spectra were analyzed using OMNIC 7.3 software.

$^{13}C-^{1}H$ HSQC 2D-NMR. For the 2D HSQC NMR experiment, around 156.6 mg of the sample was fully dissolved in 1 mL of DMSO-d_6 solvent. The spectra were recorded on Bruker Ultrashield 500 MHz plus spectrometer using hsqcetgpsisp 2.2 pulse program with other parameters: 90° pulse angle, 0.11 s acquisition time, 1.5 s pulse delay, and 16 number of scans. The $^{1}J_{CH}$ used was 145 Hz. The number of collected complex points was 1024 for the ^{1}H-dimension, and 256 increments were recorded in ^{13}C-dimension. The spectral width of 13.02 and 220.00 ppm were used for ^{1}H and ^{13}C, respectively. Data processing was performed using Mnova V.14 software.

Py-GCMS/GCMS. Pyrolysis of the lignin (L-KB) sample was performed using a CDS Pyroprobe 5200 (CDS Analytical LLC, Pennsylvania) micro-pyrolyzer. This was done by loading 1 mg of the sample into a glass pyroprobe. The pyroprobe was initially heated to 100 °C and held at that temperature for 5 s, followed by heating at 10 °C/mS to 750 °C with a 5 s hold. For GC/MS analysis, an Agilent 7890A GC/5975C gas chromatography unit was used, and the separation was made using 30 m × 0.25 mm i.d. × 0.25 mm film thickness DB-1701 mass spectroscopy column with an injection temperature of 300 °C and 70 eV electron impact. The MS scan range of m/z (mass to charge ratio) was 30−550, and the split ratio of 10:1 was used for the analysis. The GC oven temperature was held at 60 °C for 1 min and then heated to 280 °C at 15 °C/min, and the final temperature was maintained for 10 min. Helium gas was used as the carrier gas with a flow rate of 3 mL/min. The identification and analysis of the peaks were performed using the MS NIST library.

The GC-MS/FID analysis of BO-SL/L was carried out with the same instrument but without connecting the Pyroprobe. About 20 mg of bio-oil was dissolved in ∼2 g of ethanol to achieve 100× dilution, and the solution was filtered. Agilent 7890A GC/5975C gas chromatography-mass spectrometry unit was used for the analysis, with an initial temperature of 60 °C held for 1 min, and then ramping up to 280 °C at 15 °C/min, which was held for 10 min. Briefly, 3 mL/min of helium was used as a carrier gas in a DB-1701 column (30 m × 0.25 mm i.d. × 0.25 mm film thickness). The GCMS analysis of BO-FP/PW was mentioned in a previously published article.[30]

Colorimetric Quantification of Carbohydrates in Bio-Oils. The amount of carbohydrates was determined by phenol-sulfuric acid assay. Dubois et al.[35] mentioned this as a well-known colorimetric method for carbohydrates. The procedure of this method is referred to from literature[36,37] as follows. A 0.5 mL bio-oil (each bio-oil diluted with acetone as 0.01 g/mL) sample was mixed with 0.5 mL of 4% aqueous solution of phenol in a sample tube. The mixture was shaken for 30 s. Subsequently, 2.5 mL of concentrated H_2SO_4 was added to the mixture and allowed to stand for 10 min at room temperature. After that, the mixture was placed in a static water bath for another 10 min. Bio-oil samples were hydrolyzed in triplicate. Glucose standards of 0, 20, 40, and 60 μg/mL were prepared, and each standard was subjected to the hydrolysis procedure outlined above. A Genesys 150 UV−Visible spectrophotometer was used for the measurement of absorbance.

Synthesis and Characterization of NPF Resins. The NPF resins used as wood adhesives were synthesized using a 1:0.8 molar ratio of phenol to formaldehyde with 0.05 moles of oxalic acid per mole of phenol as a catalyst. Oxalic acid was selected to avoid potential corrosion to the system, as it is a weak acid.[38,39] The synthesis was conducted at 90 °C for 3 h in a four-necked flask equipped with a dropping funnel at one end for dropwise addition of the formaldehyde solution (37% formalin solution) and a condenser at another neck to prevent formaldehyde escaping through the system

https://doi.org/10.1021/acssuschemeng.1c01916
ACS Sustainable Chem. Eng. 2021, 9, 10990−11002

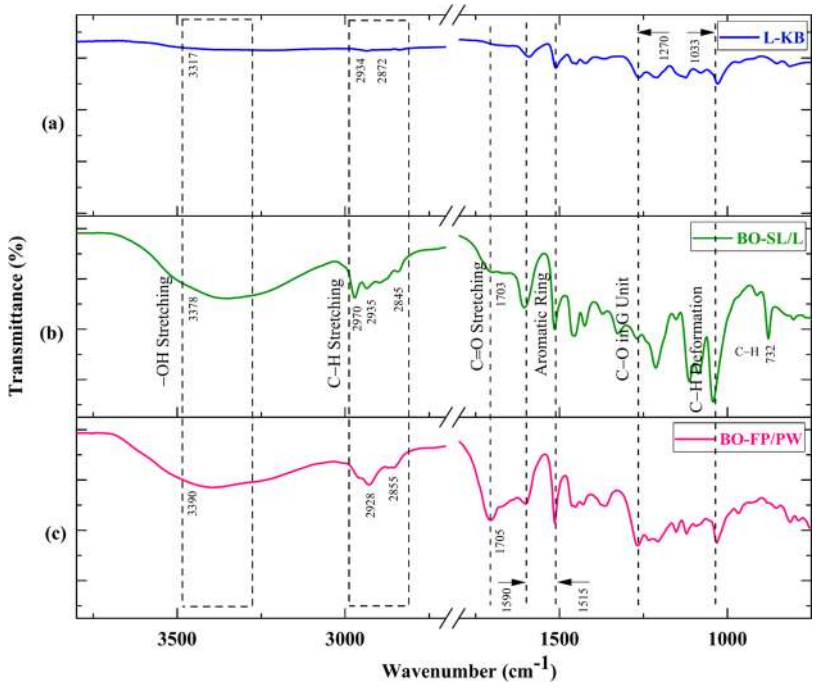

Figure 2. FTIR spectra of (a) L-KB, (b) BO-SL/L, and (c) BO-FP/PW.

at high temperature. The whole assembly was placed in a silicone oil bath to maintain a constant temperature throughout the reaction under continuous stirring. After 3 h of synthesis, the water generated as a byproduct in the reaction was removed using a rotary evaporator at 60 °C under reduced pressure to recover the PF resin. The obtained resin was labeled as 100-NPF. A similar procedure was used to synthesize resins from L-KB, BO-SL/L, and BO-FP/PW by substituting 50% (w/w) of phenol by each of the phenolic sources as described above. The synthesized resins were labeled as 50-NPF-L-KB, 50-NPF-BO-SL/L, and 50-NPF-BO-FP/PW, respectively. Further, the resins were characterized by FTIR and ^{1}H NMR spectroscopy.

^{1}H NMR Spectroscopy. The chemical structures of NPF resins were analyzed through ^{1}H NMR spectrometry using a Bruker 600 MHz NMR spectrophotometer equipped with a triple resonance cryoprobe and an automatic sample changer. Spectra were acquired by dissolving 100 mg of the sample in 1 mL of deuterated DMSO-d_6 containing 0.03% tetramethylsilane (TMS), which is used as an internal standard for referencing the chemical shifts. ^{1}H NMR spectra were recorded using 16 scans with 2.7262 s acquisition time, 1 s delay time, and 65 536 transients. Spectral data were analyzed using Mnova V.14 software.

Crosslinking of NPF Resins and Thermal Study by DSC. For the crosslinking reaction, NPF resin samples were ground with the HMTA curing agent using a mortar and pestle in the desired proportion (9% w/w HMTA/NPF resin) to achieve a homogeneous mixture. The subsequent mixture was then used for DSC analysis to study the curing properties. The combinations of each resin with HMTA were labeled as 100-NPF adhesive, 50-NPF-L-KB adhesive, 50-NPF-BO-SL/L adhesive, and 50-NPF-BO-FP/PW adhesive, respectively.

The DSC measurements were performed using a TA Q2000 (TA instruments, DE) with nitrogen purge gas at 50 mL/min. Briefly, 5−6 mg of samples were measured in DSC standard aluminum pans with a small hole punctured in the aluminum lid; the purpose of doing that was to collect the blown-out sample in the upper lid. The modulated DSC experiment was performed for each sample between 25 and 200 °C at a heating/cooling rate of 10 °C/min with two heating and cooling cycles with modulation of ±1 °C every 60 s. The first heating cycle was used to interrogate the curing phenomenon using TA instrument analysis software.

Preparation of Glued Wood Specimens. The board of southern yellow pine (*Pinus* spp.) wood was cut into eight panels of dimensions 40 × 7 × 0.035 cm^3 ($L \times W \times H$). After that, these panels were conditioned at 62% relative humidity (RH) and 22 °C temperature for 24 h. Then, the adhesive was spread uniformly to one side of the wood panel with a glue spread rate of 200 g/m^2, and the other wood panel was placed on top of it. Before application, the NPF resin was ground with HMTA (9% on weight of NPF resin), and then the homogeneous mixture was dissolved in the desired amount of acetone for ease of application on the wood substrate. In total, four glued panels were prepared corresponding to each NPF resin adhesive type using the same procedure. Afterward, all four glued wood panels were pressed at 150 °C for 15 min with 2 MPa pressure and then allowed to cool and conditioned as before. From each bonded panel, eight wood specimens were produced according to standard procedure ASTM D906-98 (2017), as illustrated in Figure 1a,b, out of which four wood specimens were used for wet shear bonding strength and physical analysis of each adhesive. The wood specimens were placed under water using a metal grid at room temperature for 24 h. After 24 h, the wood specimens were removed from the water and wiped using a paper towel.

Water Absorption (WA) and Thickness Swelling (TS). The weight and thickness of the wood specimen before immersing and after immersing in water were measured using electric balance and vernier caliper, respectively, to calculate water absorption and thickness swelling.

The water absorption (WA %) was calculated according to eq 1.[40]

$$\text{WA } \% = \frac{W_{24} - W_0}{W_0} \times 100 \quad (1)$$

where W_0 is the weight of the wood specimen before immersion and W_{24} is the weight of the wood specimen after immersing for 24 h.

The thickness swelling (TS %) of the wood specimen was calculated using eq 2.[40]

$$\text{TS } \% = \frac{T_{24} - T_0}{T_0} \times 100 \quad (2)$$

where T_0 is the average thickness taken at three different places across the wood specimen before immersion and T_{24} is the average thickness measured after immersion for 24 h.

https://doi.org/10.1021/acssuschemeng.1c01916
ACS Sustainable Chem. Eng. 2021, 9, 10990−11002

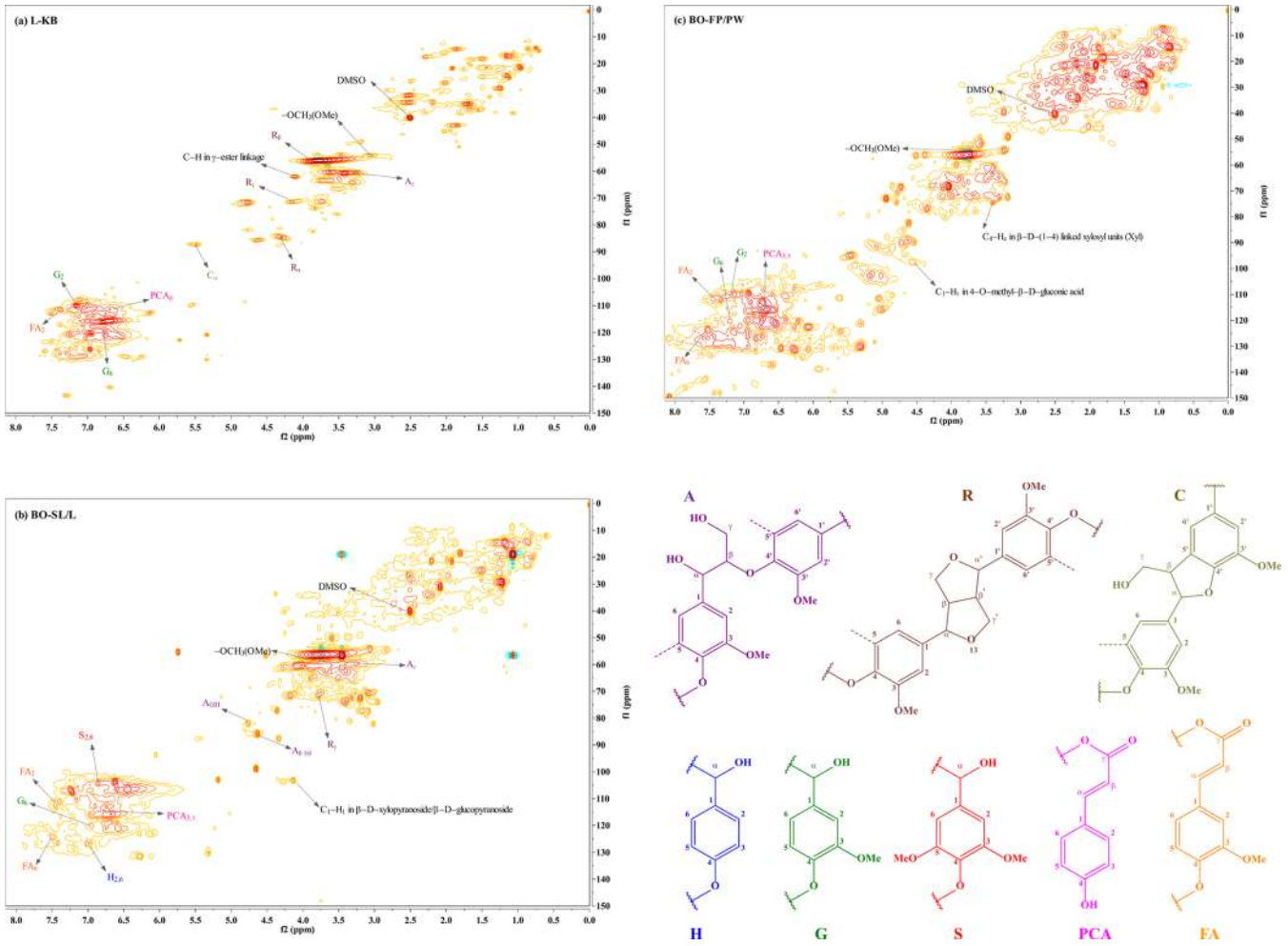

Figure 3. $^{13}C-^{1}H$ HSQC 2D-NMR spectra of (a) L-KB, (b) BO-SL/L, (c) BO-FP/PW, and possible structure present in the compounds: (A) β-O-4 (aryl ether), (R) resinol, (C) coumarate, (H) *p*-hydroxyphenyl, (G) guaiacyl, (S) syringyl, (PCA) *p*-coumarate, and (FA) ferulate.

Tensile Shear Strength. The dry and wet shear strength tests for each NPF resin adhesive were carried out following ASTM D906-98 (2017)[41] standard using an Instron 5565 universal testing machine at a constant loading speed of 1.0 mm/min and loading capacity of 10 kN.

The tensile shear strength is calculated according to eq 3.[40]

$$\text{tensile shear strength } \tau = \frac{F_{max}}{l_2 b} \quad (3)$$

where τ is the tensile shear strength (MPa), F_{max} is the maximum loading force recorded at the breaking point (N), l_2 is the length of the shear area (mm), and b is the width of the shear area (mm).

Statistical Analysis. Statistical analysis of water absorption and thickness swelling was performed using one-way analysis of variance (ANOVA) in conjunction with Tukey's post hoc test. The results were expressed as means ± standard deviations. Two-way ANOVA, followed by Tukey's post hoc test, was conducted for tensile shear strength analysis of each of the adhesives and at the dry and wet conditions. All data were analyzed using Minitab 19 software.

RESULTS AND DISCUSSION

Characterization of L-KB, BO-SL/L, and BO-FP/PW. In this study, we used lignin and bio-oils obtained from three different biorefineries. So, to understand their chemistry and structural reactivity, selective characterization was performed and presented further in the following sections.

The functional groups present in the L-KB, BO-SL/L, and BO-FP/PW were analyzed by FTIR, as shown in Figure 2. The representative peaks were assigned as per previously reported literature.[42,43] Each of them exhibited a broad peak in the region of 3500−3300 cm^{-1}, which are related to −OH stretching vibrations from phenolic and aliphatic −OH present in lignin and polysaccharides (cellulose and hemicellulose).[43] The absorption bands in the region (2900−2800 cm^{-1}) representing symmetric (νs) and asymmetric (νas) C−H stretching vibrations in CH_2 (methylene) and CH_3 (methyl) groups: 2934 cm^{-1} ($_{\nu as}CH_2$, L-KB), 2872 cm^{-1} ($_{\nu s}CH_3$, L-KB), 2970 cm^{-1} ($_{\nu as}CH_3$, BO-SL/L), 2935 cm^{-1} ($_{\nu as}CH_2$, BO-SL/L), 2845 cm^{-1} ($_{\nu s}CH_2$, BO-SL/L), 2928 cm^{-1} ($_{\nu as}CH_2$, BO-FP/PW), and 2855 cm^{-1} ($_{\nu s}CH_2$, BO-FP/PW). The BO-FP/PW and BO-SL/L have high-intensity CH_2 and CH_3 peaks, which indicates the highest proportion of CH group than L-KB. The peaks at 1703 cm^{-1} for BO-SL/L and 1705 cm^{-1} for BO-FP/PW are more likely associated with C═O stretching vibration of unconjugated ketones and carboxyl groups. The appearance of these peaks for bio-oils shows the depolymerization of lignin during the liquefaction and pyrolysis processes, which generate more carbonyl functional groups. The absorption peaks at 1590 and 1515 cm^{-1} were assigned to aromatic skeleton vibrations (guaiacyl units in LCBM). The intensity of 1270 cm^{-1} is related to the C−O stretching in guaiacyl.[44] The characteristic band for C−O−C asymmetric

https://doi.org/10.1021/acssuschemeng.1c01916
ACS Sustainable Chem. Eng. 2021, 9, 10990−11002

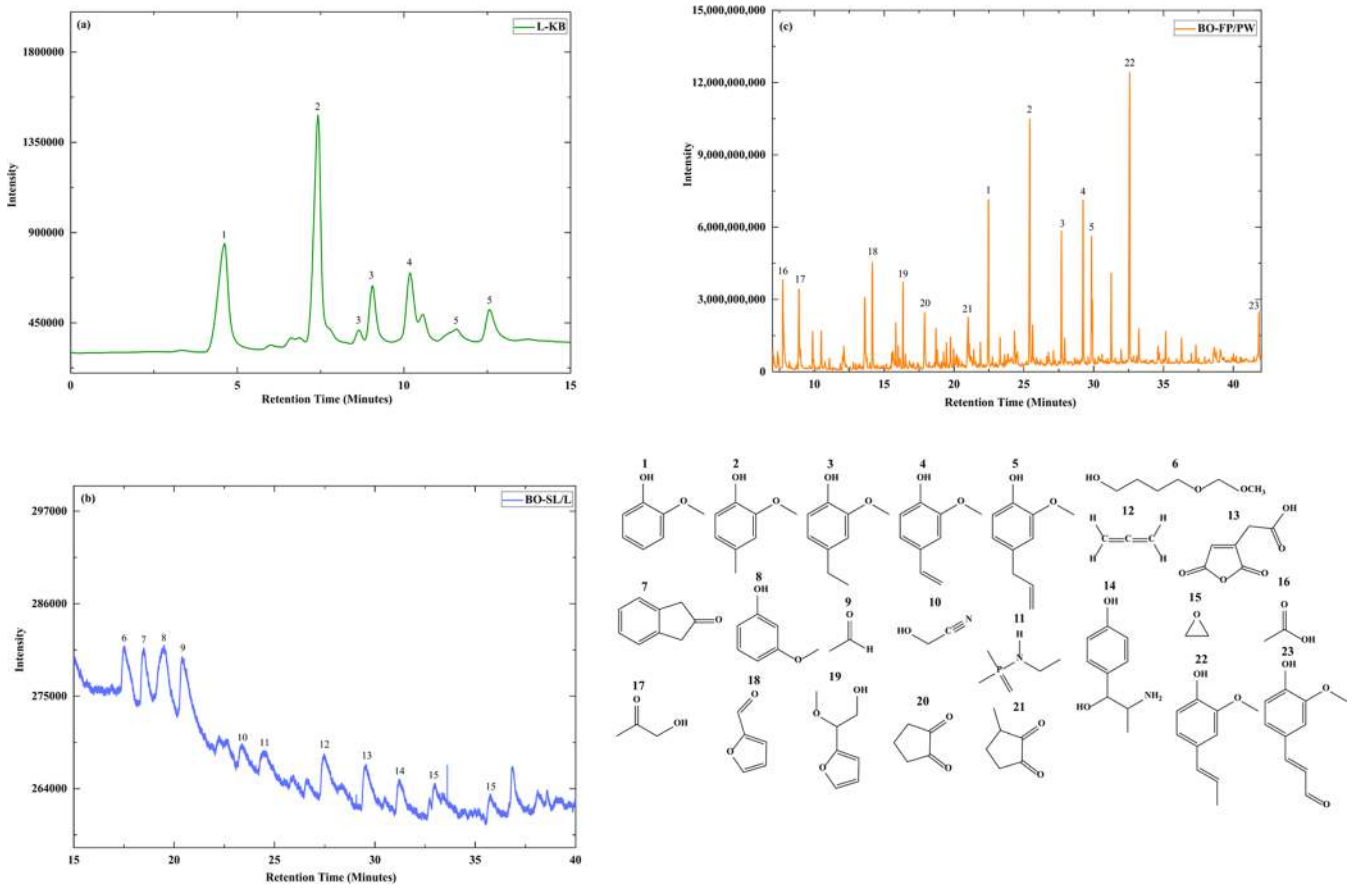

Figure 4. GCMS spectra of (a) L-KB, (b) BO-SL/L, (c) BO-FP/PW, and compounds observed in the structures.

stretching has been seen at 1152 cm^{-1} (weak) in the case of BO-FP/PW and BO-SL/L. The band detected at 1033 cm^{-1} is linked to aromatic C−H in-plane deformation in G units. A band at 732 cm^{-1} can be ascribed to the C−H out of a plane in the *p*-hydroxyl phenolic unit.

2D HSQC NMR experiment was run for L-KB, BO-SL/L, and BO-FP/PW samples, and their spectra with designated peaks and structures according to previously published articles[45] are displayed in Figure 3, which shows informative peaks in the aromatic (δC/δH 90.0−150.0/4.0−8.0), interunit aliphatic lignin (δC/δH 52.5−90.0/2.8−5.7) and aliphatic (δC/δH 8.0−52.5/0.5−4.5) region. Figure 3a represents the spectrum of L-KB. Lignin is a complex macromolecule consisting of *p*-coumaryl, coniferyl, and sinapyl alcohol. These monolignols undergo radical polymerization, forming various interunit linkages, α-O-4 (aryl ether), β-O-4 (aryl ether), β-β (pinoresinol), β-5 (phenylcoumaran), 5-5 (biphenyl), and β-1 (1,2-diaryl propane).[46] The aromatic region of kraft lignin (Figure 3a) shows strong signals related to guaiacyl (G) units at C2−H2 (δC/δH 109.5−112.8/6.7−7.2 ppm) and C6−H6 (δC/δH 118.7−121.8/6.5−7.3 ppm). This is because the kraft lignin used in this study originated from softwood. However, in the case of BO-SL/L (Figure 3b), both guaiacyl (G) and *p*-hydroxyphenyl (H) unit-related peaks were observed. In Figure 3c (BO-FP/PW), mainly guaiacyl (G) units were observed. Also, signals related to carbohydrates C_1−H_1 in 4-*O*-methyl-β-D-gluconic acid at δC/δH 97.50/4.56 were detected, which may be associated with the carbohydrates present in bio-oil.

The monomeric components present in the L-KB, BO-SL/L, and BO-FP/PW were identified using GCMS analysis as depicted in Figure 4. The L-KB lignin was subjected to pyrolysis to show GCMS peaks (Figure 4a). However, the peaks were generated through light vapors produced during pyrolysis; that is the reason why we did not observe any peaks after 15 min of retention time. The main diagnostic products shown through pyrolysis vapors are G units because the kraft lignin originated from softwood species.[47] The GCMS spectrum of BO-SL/L (Figure 4b) shows peaks of compounds produced during the depolymerization of lignin using ethanol solvent under the thermal environment. The compounds identified are alcohols, ketones, substituted phenols, and nitrogen-containing compounds.[48,49] The ester-containing compounds are generated from the esterification reaction between ethanol and acids. The substituted phenols are G and H (*p*-hydroxyphenyl) type. The bio-oil (BO-FP/PW) yield from fast pyrolysis of pinewood contains a majority of aromatic and few nonaromatic compounds, as presented in Figure 4c (GCMS spectra of BO-FP/PW). It could be seen that the phenolic compounds are mostly 2-methoxy phenol, also denoted as G units, which can be derived from pyrolytic lignin (lignin-derived fragments) present in the organic phase of bio-oil, and is also known to be prevalent in pine from softwood species.[50] Oxygenated compounds such as acids, esters, and heterocyclic organics are also detected due to breakage of side chains in lignin and decomposition of cellulose and hemicellulose.

Quantitative analysis of the carbohydrates present in the BO-SL/L and BO-FP/PW was carried out using the phenol-

https://doi.org/10.1021/acssuschemeng.1c01916
ACS Sustainable Chem. Eng. 2021, 9, 10990−11002

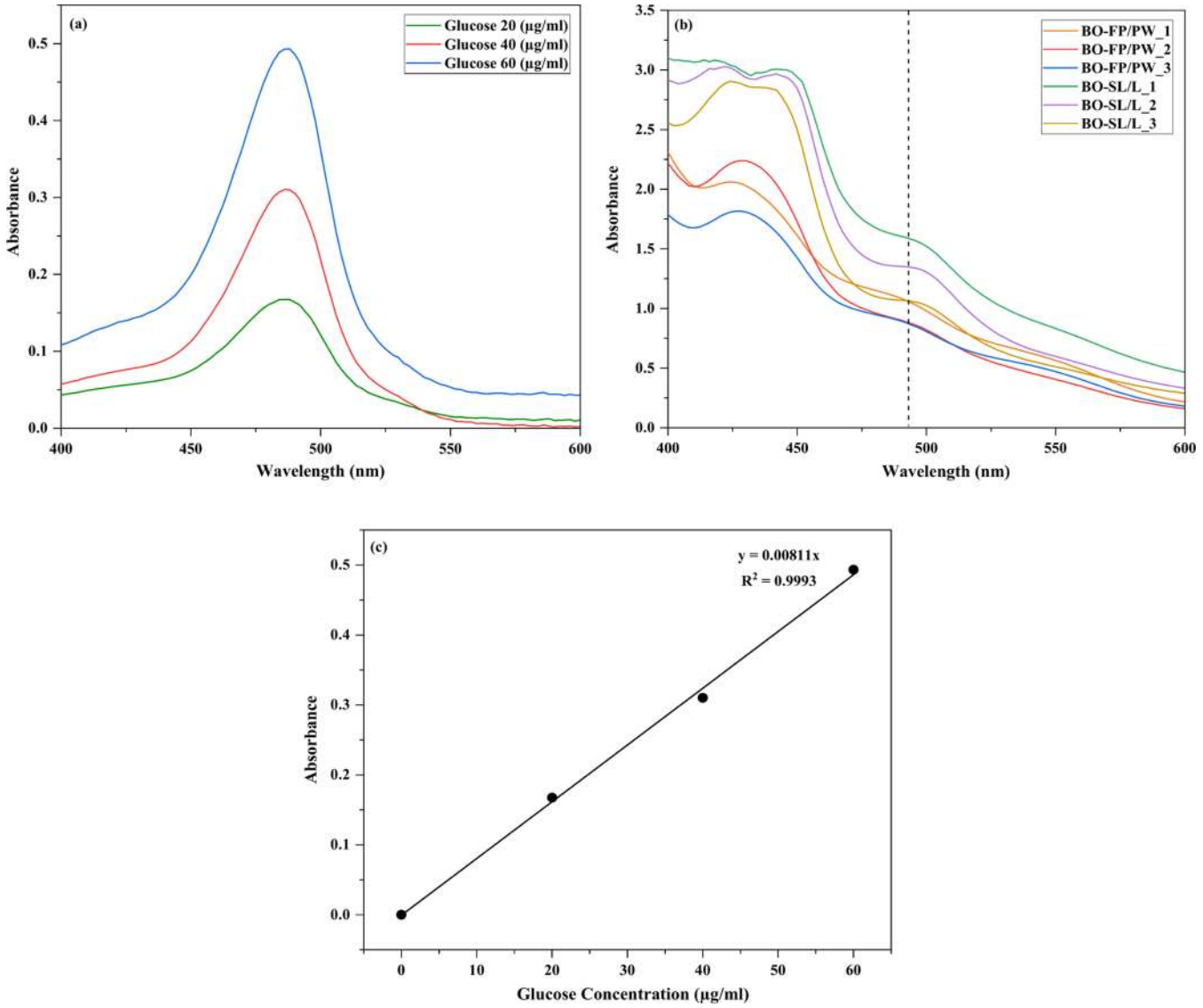

Figure 5. Carbohydrates measurement by phenol-sulfuric acid assay. (a) Ultraviolet spectra of different concentrations of glucose sugar, (b) ultraviolet spectra of bio-oils: BO-SL/L and BO-FP/PW, and (c) ultraviolet calibration curve of glucose sugar.

sulfuric acid colorimetric method. Here, in the study, glucose was used as a calibration standard, because after acid hydrolysis, the polymeric/oligomeric sugars present in the bio-oils were converted into glucose.[51,52] The absorbance maximum for glucose measured by UV−visible spectrophotometer was observed at 488 nm (Figure 5a). The generated calibration curve (Figure 5c) showed a linear relationship between absorbance and glucose concentration. Further, the calibration curve was used to measure the amount of carbohydrates in bio-oil using the maximum absorbance at 488 nm, as shown in Figure 5b.

Table 1 summarizes the carbohydrate content resulting from two bio-oils. The BO-FP/PW has an average of 24.05% of sugars in the structure. As outlined in the method, BO-FP/PW was produced from the fast pyrolysis of pinewood. During pyrolysis of biomass (pinewood), a high yield of anhydrosugars was generated through the cleavage of glycosidic bonds in cellulose.[53] However, the organic phase of bio-oil having high-polarity compounds such as sugars was used. Therefore, carbohydrates in the organic phase of BO-FP/PW could be associated with the water-insoluble sugars linked to the pyrolytic lignin. An average of 33.61% carbohydrate (sugar) was obtained for BO-SL/L, which was produced from solvent liquefaction of lignin. The authors are unaware of the source of the lignin, but the 2D HSQC spectrum (Figure 3b) provided information on the presence of ferulate units in the lignin structure. According to Ghaffar et al.,[54] lignin crosslinked with the carbohydrates via ferulate, and during liquefaction, the carbohydrates entered the bio-oil.

Table 1. Carbohydrates in Bio-Oil Analyzed by the Phenol-Sulfuric Acid Assay

	bio-oils	
	BO-SL/L	BO-FP/PW
carbohydrate content (%)	33.61 ± 6.79	24.05 ± 2.71

Characterization of NPF Resins. The four different NPF resins were prepared by polymerization reaction between reactive sites in phenol or substituted phenol and formaldehyde under the influence of temperature and catalyst. This forms methylene bridges between ortho and para sites of

https://doi.org/10.1021/acssuschemeng.1c01916
ACS Sustainable Chem. Eng. 2021, 9, 10990−11002

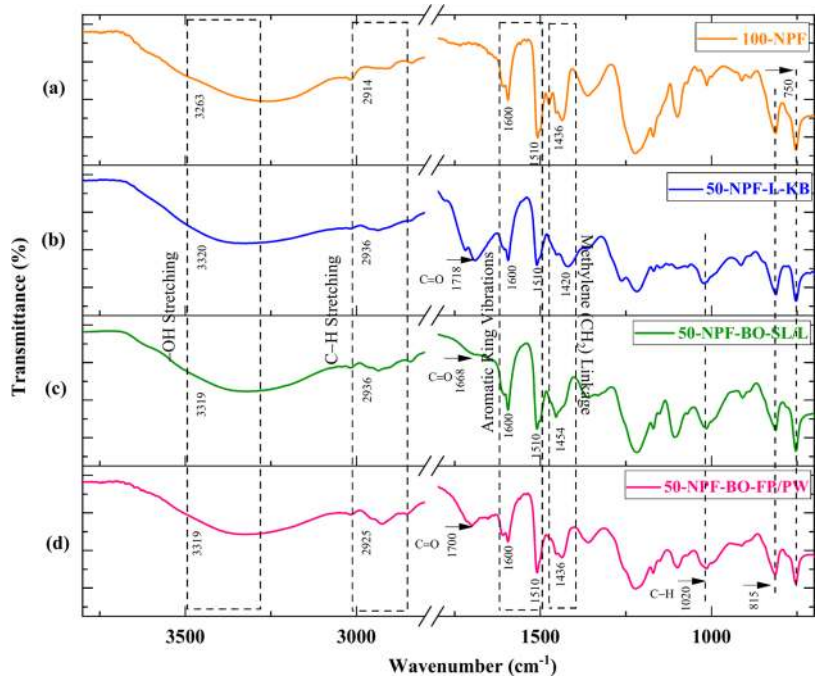

Figure 6. FTIR spectra of (a) 100-NPF, (b) 50-NPF-L-KB, (c) 50-NPF-BO-SL/L, and (d) 50-NPF-BO-FP/PW.

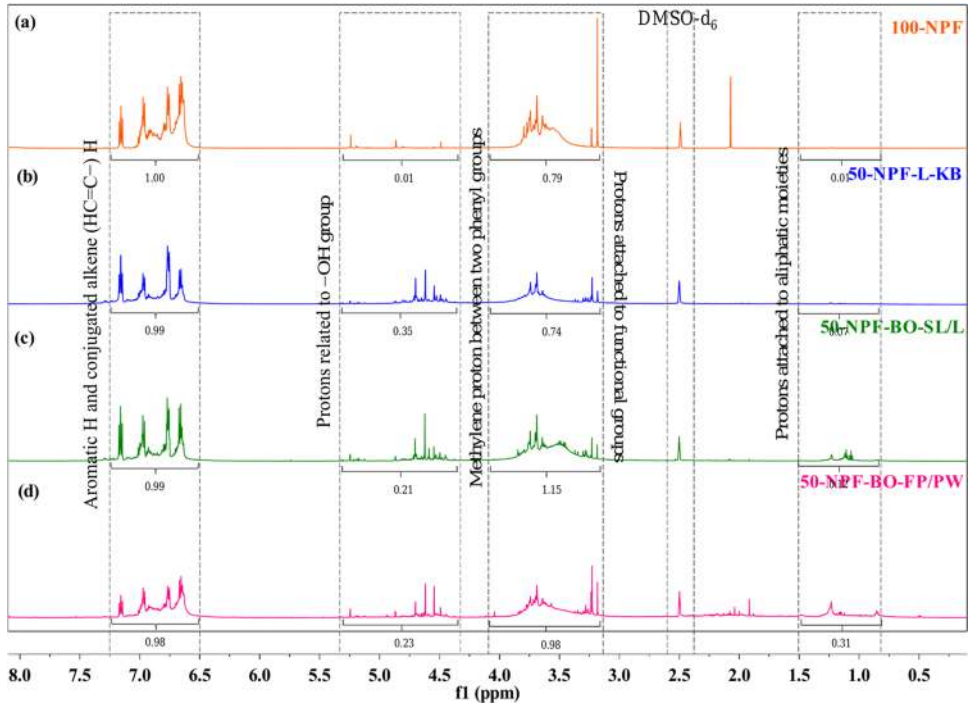

Figure 7. ^{1}H NMR spectra of (a) 100-NPF, (b) 50-NPF-L-KB, (c) 50-NPF-BO-SL/L, and (d) 50-NPF-BO-FP/PW.

phenolates in the NPF resin structure. Thus, the chemical structures of the synthesized NPF resins were investigated by FTIR and ^{1}H NMR techniques.

The FTIR spectra for 100-NPF, 50-NPF-L-KB, 50-NPF-BO-SL/L, and 50-NPF-BO-FP/PW resins are shown in Figure 6, with the respective assignment according to literature data.[55,56] The peaks between 3500 and 3300 cm^{-1} belonged to stretching vibrations of −OH present in aromatic and aliphatic hydroxyl. The peaks in the C−H stretching region were assigned to methyl/methylene (CH_3/CH_2) groups. The carbonyl peak was observed in biobased NPF resin spectra (Figure 6b−d). This was expected since the biobased NPF resins were synthesized from lignin and bio-oils. The peaks that appeared at 1600 and 1515 cm^{-1} correspond to the aromatic ring vibrations of phenyl units.[57]

The presence of signals in the region of 1470−1430 cm^{-1} confirmed the formation of a methylene bridge (CH_2) in the phenolic rings.[58] In the biobased NPF resin spectra, a peak at 1020 cm^{-1} can be seen related to the C−H deformation for the guaiacyl unit. The absorption peaks at 815 and 750 cm^{-1} were

https://doi.org/10.1021/acssuschemeng.1c01916
ACS Sustainable Chem. Eng. 2021, 9, 10990−11002

attributed to para and ortho position addition in the phenolic rings, respectively. Hpwever, the ortho position signal is more prominent in all of the spectra with oxalic acid catalyst system as proposed by Jing et al.[59]

^{1}H NMR spectra of synthesized NPF resins are presented in Figure 7. Each resin spectrum was segmented and integrated. The signal with the chemical shift of 2.5 ppm related to the DMSO-d_6 solvent. The peaks between 7.34 and 6.5 ppm are attributed to the aromatic protons of all benzene rings and unconjugated alkene protons. Signals at 5.45−4.45 ppm arose from the aliphatic and aromatic hydroxyl protons. At the same time, the high-intensity signals in this region for biobased NPF resins (Figure 7b−d) suggest the presence of aliphatic hydroxyl groups. The protons related to the methylene linkages (*o*−*o*, *o*−*p*, and *p*−*p*) formed during resin synthesis were noticed between 4.2 and 3.2 ppm. A similar observation was found in the literature for phenol−formaldehyde resins.[60−64] However, the peaks in this region overlapped with the protons from the methoxyl functional group attached to phenolic rings of G, S, and H units of LCBM.[65] The peaks in 50-NPF-BO-SL/L are more crowded, as they come from the methoxy H of syringyl units. The 2D HSQC NMR spectrum confirms the presence of syringyl units in BO-SL/L. The 50-NPF-BO-SL/L and 50-NPF-BO-FP/PW show high-intensity signals at 1.5−0.8 ppm, which might be due to the H of aliphatic side chains. The integral area ratio (peaks at 7.34−6.5 ppm to that at 4.2−3.2 ppm) for all of the NPF resins are 1:0.79 (Figure 7a), 0.99:0.71 (Figure 7b), 0.99:1.15 (Figure 7c), and 0.98:0.98 (Figure 7d). The discrepancy between the aromatic-H and methylene-H ratios was due to the overlapping of peaks.

The results from FTIR and ^{1}H NMR suggested that methylene linkages have formed during the polymerization of the respective NPF resins.

Crosslinking of the NPF Resins and Thermal Study by DSC. In general, NPF resin needs to be crosslinked by adding a curing agent, hexamethylenetetramine (HMTA). This curing process happened in two stages. In the first stage, NPF resin reacts with HMTA and forms initial intermediates such as benzoxazines and benzylamines. Further thermal decomposition of these curing intermediates generates a methylene bridge for phenolic rings.[66,67] The DSC data in Table 2 reported exothermic heat (ΔH_c) developed during the curing process of NPF resins, which is attributed to the formation of methylene bridges.

Table 2. DSC Data for NPF Resins[a]

adhesives	ΔH_c (J/g)	T_p (°C)
100-NPF adhesive	36.31	137.53
50-NPF-L-KB adhesive	31.85	138.59
50-NPF-BO-SL/L adhesive	14.51	141.31
50-NPF-BO-FP/PW adhesive	19.68	140.98

[a]ΔH_c = curing exotherm enthalpy and T_p = curing peak temperature.

The biobased NPF adhesive exhibited different curing properties from the 100-NPF adhesive. The decrease in ΔH_c (31.85, 14.51, and 19.68 J/g) was evident when 50% (w/w) of phenol was replaced by L-KB, BO-SL/L, and BO-FP/PW, respectively, which could be due to the lower chemical reactivity of the phenolic rings in the LCBM structure causing steric hindrance during the curing process. The same observation may be connected with curing peak temperature (T_p) of biobased NPF adhesive. However, compared to the data in Table 2, the 50-NPF-L-KB adhesive has similar values of ΔH_c and T_p as the 100-NPF adhesive, which suggests that L-KB has more accessible sites in the structure for the curing process compared to the bio-oils, which the previous characterization has confirmed. The endothermic peak (Figure 8) observed during the curing process might be due to the condensation reaction of the methylol group with phenol.

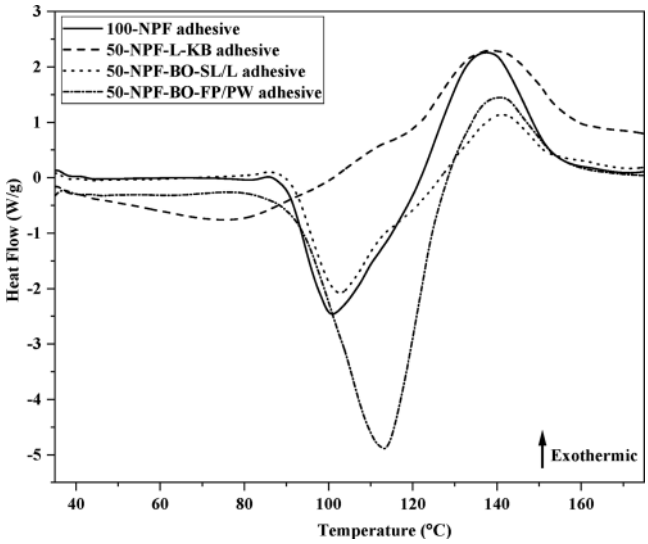

Figure 8. DSC thermograms of the NPF resin adhesives.

Bonding Performance of NPF Resin Adhesives on Wood Substrates. *Water Absorption and Thickness Swelling.* One of the main concerns in applying wood adhesives for exterior applications is the impact of water or humid environment on the wood bonding. To understand the effect, we have measured the mass and thickness gain of the wood panels after soaking in water for 24 h, and the values are listed in Table 3. The result showed that the WA values of the biobased NPF resins are relatively high. Among them, the wood samples glued with 50-BO-FP/PW adhesive absorbed more water compared to other adhesives ($p < 0.05$, Table 3). This behavior may be correlated with carbohydrates (sugar) in the structure (as evidenced by Table 1). The same observation can be valid for 50-NPF-BO-SL/L adhesive glued wood. At the same time, the 43.96% of WA in 50-NPF-L-KB was due to the hydroxyl group in the lignin. Similar results were also observed in another biobased adhesive in the literature.[68,69]

Table 3. Water Absorption (WA %) and Thickness Swelling (% TS) of the Wood Specimens Prepared with Different Adhesives[a]

	mean ± standard deviation	
adhesives	water absorption (%)	% thickness swelling
100-NPF adhesive	42.80 ± 1.25 b	11.15 ± 2.94 a
50-NPF-L-KB adhesive	43.96 ± 2.72 b	07.95 ± 1.08 b
50-NPF-BO-SL/L adhesive	43.06 ± 2.55 b	09.01 ± 2.53 ab
50-NPF-BO-FP/PW adhesive	49.00 ± 1.64 a	11.04 ± 1.71 a

[a]Water absorption (WA %) and thickness swelling (% TS) of the glued wood specimens were analyzed with one-way ANOVA, followed by Tukey's post hoc test. Different letters for each column represent significantly different water absorption and thickness swelling, respectively ($p < 0.05$).

https://doi.org/10.1021/acssuschemeng.1c01916
ACS Sustainable Chem. Eng. 2021, 9, 10990−11002

The thickness swelling data in Table 3 displays the clear evidence of dimensional change of wood matrix due to interaction of hydrophilic group present in the adhesive with the water molecule. In contrast, the wood sample bonded with the 100-NPF adhesive showed a high TS value ($p < 0.05$, Table 3); this might have been due to the penetration of water into the voids of the wood itself.[70]

Tensile Shear Strength. Tensile shear strength (wet and dry) has been conducted on each glued wood sample and presented in Figure 9. There was no significant difference

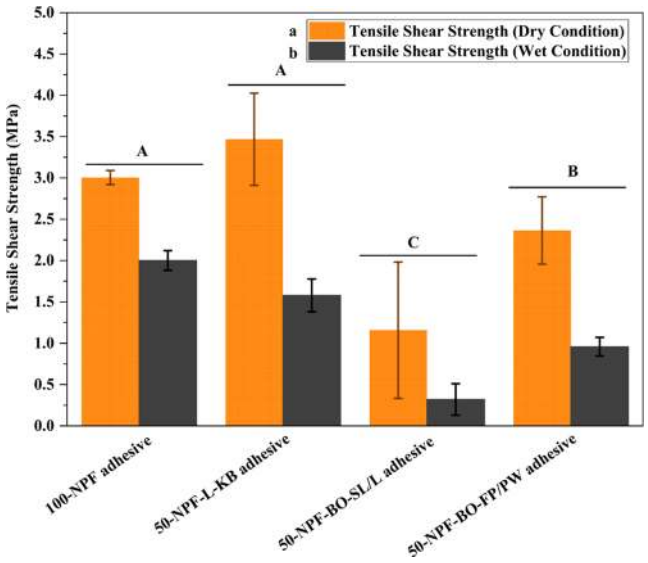

Figure 9. Dry and wet shear bonding strength of the wood specimens bonded with different adhesives: 100-NPF adhesive, 50-NPF-L-KB adhesive, 50-NPF-BO-SL/L adhesive, and 50-NPF-BO-FP/PW adhesive. Four wood samples per adhesive for each strength measurement were prepared. The data are the means of five replicates, and the error bars represent standard deviation (SD). The obtained adhesion data was analyzed using two-way ANOVA, followed by Tukey's post hoc test. Different letters on the bar represent significantly different adhesion strengths ($p < 0.05$).

found between the wood specimens bonded with 100-NPF and 50-NPF-L-KB adhesive ($p > 0.05$, Figure 9). This suggests that there is a benefit in replacing 50% of phenol with kraft biorefinery-obtained lignin. The 50-NPF-L-KB adhesive glued wood product gave the highest strength (3.46 ± 0.55 MPa) among all of the tested adhesives. This high adhesion strength could be ascribed to the functional macromolecular structure of lignin having high molar mass (as reported in Table S1), which facilitates the bonding with the wood substrate during the curing process. This observation is in good agreement with the literature reported for lignin-based wood adhesives.[24,71,72] Furthermore, the bonding strength of wood samples pressed with 50-NPF-BO-SL/L and 50-NPF-BO-FP/PW adhesives was significantly lower than that of samples pressedwith the 50-NPF-L-KB adhesive ($p < 0.05$, Figure 9). The possible reason should be that along with phenolic compounds (H, G, and S units), other compounds such as aliphatic fractions and carbohydrates are detected in the bio-oils, as discussed in characterization, limiting the reactivity and interaction between functional groups in the resin.[73,74]

Regarding wet strength, after soaking in water for 24 h, the strength of all glued samples drastically decreased ($p < 0.05$, Figure 9). This would be because the cohesion within the adhesive is destroyed by absorbed moisture. Overall, the shear strength values obtained at dry and wet conditions can meet the standard specified by the Engineered Wood Association (APA) except for 50-NPF-BO-SL/L adhesive at the wet condition.

CONCLUSIONS

This experimental work represents different biorefinery approaches to produce phenolic sources (L-KB, BO-SL/L, and BO-FP/PW) substitution to develop wood adhesives. The structure of these LCBM phenolic sources was analyzed using FTIR, $^{13}C-^{1}H$ HSQC 2D-NMR, GCMS, and carbohydrate analysis techniques. The 2D-NMR and GCMS results demonstrate that most "G-type" units are present in every structure that makes them suitable for NPF resin synthesis. Using FTIR and ^{1}H-NMR, it was possible to explain that the NPF resins are successfully synthesized, forming methylene linkages in their structures. DSC analysis was used to investigate the curing process of the NPF resin, and with the generated data, we designed an optimized curing temperature for wood bonding. The ANOVA results clarified a statistically significant difference between the bonding strength of biobased NPF resin adhesives. The dry bonding strength of all NPF resins was significantly higher than the wet bonding strength. Overall, the lignin derived from kraft biorefinery (L-KB) was the appropriate substitute for petroleum-based phenol in NPF resin synthesis because it shows high bonding strength with moderate curing energy.

ASSOCIATED CONTENT

Supporting Information

The Supporting Information is available free of charge at https://pubs.acs.org/doi/10.1021/acssuschemeng.1c01916.

GPC analysis and acetylation of L-KB, FTIR spectra of (a) L-KB and (b) acetylated L-KB (Figure S1), and molecular weight by GPC (Table S1) (PDF)

AUTHOR INFORMATION

Corresponding Author

Maria L. Auad − *Center for Polymers and Advanced Composites, Gavin Engineering Research Laboratory, Auburn University, Auburn, Alabama 36849, United States; Department of Chemical Engineering, Auburn University, Auburn, Alabama 36849, United States;* orcid.org/0000-0001-6932-5645; Phone: +1334-844-5459; Email: auad@auburn.edu

Authors

Archana Bansode − *Center for Polymers and Advanced Composites, Gavin Engineering Research Laboratory, Auburn University, Auburn, Alabama 36849, United States; Department of Chemical Engineering, Auburn University, Auburn, Alabama 36849, United States*

Mehul Barde − *Center for Polymers and Advanced Composites, Gavin Engineering Research Laboratory, Auburn University, Auburn, Alabama 36849, United States; Department of Chemical Engineering, Auburn University, Auburn, Alabama 36849, United States*

Osei Asafu-Adjaye − *Forest Products Development Center, Auburn University, Auburn, Alabama 36849, United States*

Vivek Patil − *Department of Biosystems Engineering, Auburn University, Auburn, Alabama 36849, United States;* orcid.org/0000-0003-3381-6498
John Hinkle − *Center for Polymers and Advanced Composites, Gavin Engineering Research Laboratory, Auburn University, Auburn, Alabama 36849, United States; Department of Chemical Engineering, Auburn University, Auburn, Alabama 36849, United States*
Brian K. Via − *Forest Products Development Center, Auburn University, Auburn, Alabama 36849, United States*
Sushil Adhikari − *Department of Biosystems Engineering, Auburn University, Auburn, Alabama 36849, United States;* orcid.org/0000-0002-6539-6822
Andrew J. Adamczyk − *Department of Chemical Engineering, Auburn University, Auburn, Alabama 36849, United States*
Ramsis Farag − *Center for Polymers and Advanced Composites, Gavin Engineering Research Laboratory, Auburn University, Auburn, Alabama 36849, United States; Department of Chemical Engineering, Auburn University, Auburn, Alabama 36849, United States*
Thomas Elder − *USDA-Forest Service, Southern Research Station, Auburn University, Auburn, Alabama 36849, United States*
Nicole Labbé − *Center for Renewable Carbon, University of Tennessee, Knoxville, Tennessee 37996, United States;* orcid.org/0000-0002-2117-4259

Complete contact information is available at: https://pubs.acs.org/10.1021/acssuschemeng.1c01916

Notes

The authors declare no competing financial interest.

■ ACKNOWLEDGMENTS

The authors would like to acknowledge the NSF-CREST Center for Sustainable Lightweight Materials (C-SLAM) award no. 1735971 and the USDA Grant 18-JV-11330131-073 for funding this study. Dr. Beatriz Vega from Auburn University is acknowledged for helping with the colorimetric experiment.

■ REFERENCES

(1) Pizzi, A.; Mittal, K. L. *Handbook of Adhesive Technology*, 3rd ed.; CRC Press: Boca Raton, FL, 2018, p 2544.
(2) López, F. J. D.; Montalvo, C. A Comprehensive Review of the Evolving and Cumulative Nature of Eco-Innovation in the Chemical Industry. *J. Cleaner Prod.* **2015**, *102*, 30−43.
(3) Cherubini, F. The Biorefinery Concept: Using Biomass Instead of Oil for Producing Energy and Chemicals. *Energy Convers. Manage.* **2010**, *51*, 1412−1421.
(4) Takkellapati, S.; Li, T.; Gonzalez, M. A. An Overview of Biorefinery-Derived Platform Chemicals from a Cellulose and Hemicellulose Biorefinery. *Clean Technol. Environ. Policy* **2018**, *20*, 1615−1630.
(5) Limayem, A.; Ricke, S. C. Lignocellulosic Biomass for Bioethanol Production: Current Perspectives, Potential Issues and Future Prospects. *Prog. Energy Combust. Sci.* **2012**, *38*, 449−467.
(6) Hu, J.; Zhang, Q.; Lee, D. J. Kraft Lignin Biorefinery: A Perspective. *Bioresour. Technol.* **2018**, *247*, 1181−1183.
(7) Azadi, P.; Inderwildi, O. R.; Farnood, R.; King, D. A. Liquid Fuels, Hydrogen and Chemicals from Lignin: A Critical Review. *Renewable Sustainable Energy Rev.* **2013**, *21*, 506−523.
(8) Kouisni, L.; Gagné, A.; Maki, K.; Holt-Hindle, P.; Paleologou, M. LignoForce System for the Recovery of Lignin from Black Liquor: Feedstock Options, Odor Profile, and Product Characterization. *ACS Sustainable Chem. Eng.* **2016**, *4*, 5152−5159.
(9) Lake, M. A.; Blackburn, J. C. SLRP - An Innovative Lignin-Recovery Technology. *Cellul. Chem. Technol.* **2014**, *48*, 799−804.
(10) Richter, A. P.; Bharti, B.; Armstrong, H. B.; Brown, J. S.; Plemmons, D.; Paunov, V. N.; Stoyanov, S. D.; Velev, O. D. Synthesis and Characterization of Biodegradable Lignin Nanoparticles with Tunable Surface Properties. *Langmuir* **2016**, *32*, 6468−6477.
(11) Xiaolei Zhang, R. C. B. Introduction to Thermochemical Processing of Biomass into Fuels, Chemicals, and Power. In *THERMOCHEMICAL PROCESSING OF BIOMASS : conversion into fuels, chemicals and power*, Brown, R. C., Ed.; John Wiley & Sons Ltd, **2019**, pp 1−16.
(12) Doassans-Carrère, N.; Ferrasse, J. H.; Boutin, O.; Mauviel, G.; Lédé, J. Comparative Study of Biomass Fast Pyrolysis and Direct Liquefaction for Bio-Oils Production: Products Yield and Characterizations. *Energy Fuels* **2014**, *28*, 5103−5111.
(13) Brand, S.; Hardi, F.; Kim, J.; Suh, D. J. Effect of Heating Rate on Biomass Liquefaction: Differences between Subcritical Water and Supercritical Ethanol. *Energy* **2014**, *68*, 420−427.
(14) Arpa Ghosh, M. R. H. Solvent Liquefaction. In *Thermochemical Processing of Biomass: Conversion into Fuels, Chemicals and Power*, 2nd ed.; Brown, R. C., Ed.; John Wiley & Sons, 2019; pp 257−306.
(15) Kim, J.; Won, H.; Min, S.; Jae, J.; Park, Y. Bioresource Technology Overview of the Recent Advances in Lignocellulose Liquefaction for Producing Biofuels, Bio-Based Materials and Chemicals. *Bioresour. Technol.* **2019**, *279*, 373−384.
(16) Kirtania, K. Thermochemical Conversion Processes for Waste Biorefinery. In *Waste Biorefinery: Potential and Perspectives*; Bhaskar, T.; Pandey, A.; Mohan, S. V.; Lee, D.-J.; Khanal, S. K., Eds.; Elsevier, 2018; pp 129−156.
(17) Chiaramonti, D.; Prussi, M.; Buffi, M.; Rizzo, A. M.; Pari, L. Review and Experimental Study on Pyrolysis and Hydrothermal Liquefaction of Microalgae for Biofuel Production. *Appl. Energy* **2017**, *185*, 963−972.
(18) Balat, M.; Balat, M.; Kirtay, E.; Balat, H. Main Routes for the Thermo-Conversion of Biomass into Fuels and Chemicals. Part 1: Pyrolysis Systems. *Energy Convers. Manage.* **2009**, *50*, 3147−3157.
(19) Alsbou, E.; Helleur, B. Accelerated Aging of Bio-Oil from Fast Pyrolysis of Hardwood. *Energy Fuels* **2014**, *28*, 3224−3235.
(20) Mohan, D.; Pittman, C. U.; Steele, P. H. Pyrolysis of Wood/Biomass for Bio-Oil: A Critical Review. *Energy Fuels* **2006**, *20*, 848−889.
(21) Effendi, A.; Gerhauser, H.; Bridgwater, A. V. Production of Renewable Phenolic Resins by Thermochemical Conversion of Biomass: A Review. *Renewable Sustainable Energy Rev.* **2008**, *12*, 2092−2116.
(22) Hocking, M. B. Commercial Polycondensation (Step-Growth) Polymers. *Handb. Chem. Technol. Pollut. Control* **2005**, 689−712.
(23) Granado, L.; Tavernier, R.; Henry, S.; Auke, R. O.; Foyer, G.; David, G.; Caillol, S. Toward Sustainable Phenolic Thermosets with High Thermal Performances. *ACS Sustainable Chem. Eng.* **2019**, *7*, 7209−7217.
(24) Wang, L.; Lagerquist, L.; Zhang, Y.; Koppolu, R.; Tirri, T.; Sulaeva, I.; von Schoultz, S.; Vähäsalo, L.; Pranovich, A.; Rosenau, T.; et al. Tailored Thermosetting Wood Adhesive Based on Well-Defined Hardwood Lignin Fractions. *ACS Sustainable Chem. Eng.* **2020**, *8*, 13517−13526.
(25) Kalami, S.; Arefmanesh, M.; Master, E.; Nejad, M. Replacing 100% of Phenol in Phenolic Adhesive Formulations with Lignin. *J. Appl. Polym. Sci.* **2017**, No. 45124.
(26) Jin, Y.; Cheng, X.; Zheng, Z. Preparation and Characterization of Phenol-Formaldehyde Adhesives Modified with Enzymatic Hydrolysis Lignin. *Bioresour. Technol.* **2010**, *101*, 2046−2048.
(27) Sarika, P. R.; Nancarrow, P.; Khansaheb, A.; Ibrahim, T. Bio-Based Alternatives to Phenol and Formaldehyde for the Production of Resins. *Polymers* **2020**, No. 2237.
(28) Yan, N.; Zhang, B.; Zhao, Y.; Farnood, R. R.; Shi, J. Application of Biobased Phenol Formaldehyde Novolac Resin Derived from

Beetle Infested Lodgepole Pine Barks for Thermal Molding of Wood Composites. *Ind. Eng. Chem. Res.* **2017**, *56*, 6369−6377.
(29) Pan, H. Wood Liquefaction in the Presence of Phenol with a Weak Acid Catalyst and Its Potential for Novolac Type Wood Adhesives. Ph.D. Dissertation, Louisiana State University and Agricultural and Mechanical College, Baton Rouge, LA, 2007.
(30) Barde, M.; Edmunds, C. W.; Labbé, N.; Auad, M. L. Fast Pyrolysis Bio-Oil from Lignocellulosic Biomass for the Development of Bio-Based Cyanate Esters and Cross-Linked Networks. *High Perform. Polym.* **2019**, *31*, 1140−1152.
(31) Fan, D.; Xie, X.; Li, Y.; Li, L.; Sun, J. Aromatic Compounds from Lignin Liquefaction over ZSM-5 Catalysts in Supercritical Ethanol. *Chem. Eng. Technol.* **2018**, *41*, 509−516.
(32) Nandiwale, K. Y.; Danby, A. M.; Ramanathan, A.; Chaudhari, R. V.; Subramaniam, B. Dual Function Lewis Acid Catalyzed Depolymerization of Industrial Corn Stover Lignin into Stable Monomeric Phenols. *ACS Sustainable Chem. Eng.* **2019**, *7*, 1362−1371.
(33) Kim, P.; Weaver, S.; Noh, K.; Labbé, N. Characteristics of Bio-Oils Produced by an Intermediate Semipilot Scale Pyrolysis Auger Reactor Equipped with Multistage Condensers. *Energy Fuels* **2014**, *28*, 6966−6973.
(34) Barde, M.; Avery, K.; Edmunds, C. W.; Labbé, N.; Auad, M. L. Cross-Linked Acrylic Polymers from the Aqueous Phase of Biomass Pyrolysis Oil and Acrylated Epoxidized Soybean Oil. *ACS Sustainable Chem. Eng.* **2019**, *7*, 2216−2224.
(35) Dubois, M.; Gilles, K. A.; Hamilton, J. K.; Rebers, P. A.; Smith, F. Colorimetric Method for Determination of Sugars and Related Substances. *Anal. Chem.* **1956**, *28* (3), 350−356.
(36) Albalasmeh, A. A.; Berhe, A. A.; Ghezzehei, T. A. A New Method for Rapid Determination of Carbohydrate and Total Carbon Concentrations Using UV Spectrophotometry. *Carbohydr. Polym.* **2013**, *97*, 253−261.
(37) Fournier, E. Colorimetric Quantification Of Carbohydrates. *Handb. Food Anal. Chem.* **2005**, *1*−*2*, 653−660.
(38) Conner, A. Wood: Adhesives. In *Encyclopedia of Materials: Science and Technology*; Elsevier Science, Ltd., 2001; p 17.
(39) Jing, Z.; Lihong, H.; Bingchuan, L.; Caiying, B.; Puyou, J.; Yonghong, Z. Preparation and Characterization of Novolac Phenol-Formaldehyde Resins with Enzymatic Hydrolysis Lignin. *J. Taiwan Inst. Chem. Eng.* **2015**, 178−182.
(40) Efhamisisi, D.; Thevenon, M. F.; Hamzeh, Y.; Karimi, A. N.; Pizzi, A.; Pourtahmasi, K. Induced Tannin Adhesive by Boric Acid Addition and Its Effect on Bonding Quality and Biological Performance of Poplar Plywood. *ACS Sustainable Chem. Eng.* **2016**, *4*, 2734−2740.
(41) Conshohocken, W. Standard Test Method for Strength Properties of Adhesives in Plywood Type Construction in Shear by Tension Loading 1. *ASTM*, **2017**, *i*, 1 4. DOI: 10.1520/D0906-20.responsibility.
(42) Passauer, L.; Salzwedel, K.; Struch, M.; Herold, N.; Appelt, J. Quantitative Analysis of the Etherification Degree of Phenolic Hydroxyl Groups in Oxyethylated Lignins: Correlation of Selective Aminolysis with FTIR Spectroscopy. *ACS Sustainable Chem. Eng.* **2016**, *4*, 6629−6637.
(43) Moghaddam, L.; Rencoret, J.; Maliger, V. R.; Rackemann, D. W.; Harrison, M. D.; Gutiérrez, A.; Del Río, J. C.; Doherty, W. O. S. Structural Characteristics of Bagasse Furfural Residue and Its Lignin Component. An NMR, Py-GC/MS, and FTIR Study. *ACS Sustainable Chem. Eng.* **2017**, *5*, 4846−4855.
(44) Zhao, J.; Xiuwen, W.; Hu, J.; Liu, Q.; Shen, D.; Xiao, R. Thermal Degradation of Softwood Lignin and Hardwood Lignin by TG-FTIR and Py-GC/MS. *Polym. Degrad. Stab.* **2014**, *108*, 133−138.
(45) Rencoret, J.; Prinsen, P.; Gutiérrez, A.; Martínez, Á. T.; del Río, J. C. Isolation and Structural Characterization of the Milled Wood Lignin, Dioxane Lignin, and Cellulolytic Lignin Preparations from Brewer's Spent Grain. *J. Agric. Food Chem.* **2015**, *63*, 603−613.
(46) Glasser, W. G. About Making Lignin Great Again—Some Lessons From the Past. *Front. Chem.* **2019**, No. 565.
(47) Hita, I.; Heeres, H. J.; Deuss, P. J. Insight into Structure−Reactivity Relationships for the Iron-Catalyzed Hydrotreatment of Technical Lignins. *Bioresour. Technol.* **2018**, *267*, 93−101.
(48) Leng, L.; Zhang, W.; Peng, H.; Li, H.; Jiang, S.; Huang, H. Nitrogen in Bio-Oil Produced from Hydrothermal Liquefaction of Biomass: A Review. *Chem. Eng. J.* **2020**, *401*, No. 126030.
(49) Guo, K.; Cheng, Q.; Jiang, J.; Xu, J.; Tan, W. Qualitative Analysis of Liquid Products Generated from Lignocellulosic Biomass Using Post-Target and Nontarget Analysis Methods and Liquefaction Mechanism Research. *ACS Sustainable Chem. Eng.* **2020**, 11099−11113.
(50) Vitasari, C. R.; Meindersma, G. W.; de Haan, A. B. Water Extraction of Pyrolysis Oil: The First Step for the Recovery of Renewable Chemicals. *Bioresour. Technol.* **2011**, *102*, 7204−7210.
(51) Johnston, P. A.; Brown, R. C. Quantitation of Sugar Content in Pyrolysis Liquids after Acid Hydrolysis Using High-Performance Liquid Chromatography without Neutralization. *J. Agric. Food Chem.* **2014**, *62*, 8129−8133.
(52) Rover, M. R. Analysis of Sugars and Phenolic Compounds in Bio-Oil. Ph.D. Dissertation, Iowa State University, 2013.
(53) Yu, Y.; Chua, Y. W.; Wu, H. Characterization of Pyrolytic Sugars in Bio-Oil Produced from Biomass Fast Pyrolysis. *Energy Fuels* **2016**, *30*, 4145−4149.
(54) Ghaffar, S. H.; Fan, M. Structural Analysis for Lignin Characteristics in Biomass Straw. *Biomass Bioenergy* **2013**, *57*, 264−279.
(55) Dante, R. C.; Santamaria, D. A.; Gil, J. M. Crosslinking and Thermal Stability of Thermosets Based on Novolak and Melamine. *J. Appl. Polym. Sci.* **2009**, *114*, 4059−4065.
(56) Kumar, H.; Tripathi, S. K.; Mistry, S.; Bajpai, G. Synthesis, Characterization and Application of Coatings Based on Epoxy Novolac and Liquid Rubber Blend. *E-J. Chem.* **2009**, *6*, 1253−1259.
(57) Guo, Z.; Liu, Z.; Ye, L.; Ge, K.; Zhao, T. The Production of Lignin-Phenol-Formaldehyde Resin Derived Carbon Fibers Stabilized by BN Preceramic Polymer. *Mater. Lett.* **2015**, *142*, 49−51.
(58) Chen, Y.; Chen, Z.; Xiao, S.; Liu, H. A Novel Thermal Degradation Mechanism of Phenol-Formaldehyde Type Resins. *Thermochim. Acta* **2008**, *476*, 39−43.
(59) Jing, Z.; Lihong, H.; Bingchuan, L.; Caiying, B.; Puyou, J.; Yonghong, Z. Preparation and Characterization of Novolac Phenol-Formaldehyde Resins with Enzymatic Hydrolysis Lignin. *J. Taiwan Inst. Chem. Eng.* **2015**, *54*, 178−182.
(60) Koley, R.; Kasilingam, R.; Sahoo, S.; Chattopadhyay, S.; Bhowmick, A. K. Synthesis and Characterization of Phenol Furfural Resin from Moringa Oleifera Gum and Biophenol and Its Application in Styrene Butadiene Rubber. *Ind. Eng. Chem. Res.* **2019**, *58*, 18519−18532.
(61) Yelle, D. J.; Ralph, J. Characterizing Phenol-Formaldehyde Adhesive Cure Chemistry within the Wood Cell Wall. *Int. J. Adhes. Adhes.* **2016**, *70*, 26−36.
(62) Huang, J.; Xu, M.; Ge, Q.; Lin, M.; Lin, Q.; Chen, Y.; Chu, J.; Dai, L.; Zou, Y. Controlled Synthesis of High-Ortho-Substitution Phenol-Formaldehyde Resins. *J. Appl. Polym. Sci.* **2005**, *97*, 652−658.
(63) Kandola, B. K.; Krishnan, L.; Deli, D.; Luangtriratana, P.; Ebdon, J. R. Fire and Mechanical Properties of a Novel Free-Radically Cured Phenolic Resin Based on a Methacrylate-Functional Novolac and of Its Blends with an Unsaturated Polyester Resin. *RSC Adv.* **2015**, *5*, 33772−33785.
(64) Scariah, K. J.; Usha, K. M.; Narayanaswamy, K.; Shanmugam, K.; Sastri, K. S. Evaluation of Isomeric Composition of Resol-Type Phenol Formaldehyde Matrix Resins for Silica-Phenolic Composites and Its Effect on Cure Characteristics of the Resin. *J. Appl. Polym. Sci.* **2003**, 2517−2524.
(65) Wang, Y.; Wang, S.; Leng, F.; Chen, J.; Zhu, L.; Luo, Z. Separation and Characterization of Pyrolytic Lignins from the Heavy Fraction of Bio-Oil by Molecular Distillation. *Sep. Purif. Technol.* **2015**, *152*, 123−132.

(66) Patel, J. P.; Xiang, Z. G.; Hsu, S. L.; Schoch, A. B.; Carleen, S. A.; Matsumoto, D. Characterization of the Crosslinking Reaction in High Performance Adhesives. *Int. J. Adhes. Adhes.* **2017**, *78*, 256−262.
(67) Wang, L.; Lagerquist, L.; Zhang, Y.; Koppolu, R.; Tirri, T.; Sulaeva, I.; von Schoultz, S.; Vahasalo, L.; Pranovich, A.; Rosenau, T.; et al. Tailored Thermosetting Wood Adhesive Based on Well-Defined Hardwood Lignin Fractions. *ACS Sustainable Chem. Eng.* **2020**, 13517−13526.
(68) Mekonnen, T. H.; Mussone, P. G.; Choi, P.; Bressler, D. C. Adhesives from Waste Protein Biomass for Oriented Strand Board Composites: Development and Performance. *Macromol. Mater. Eng.* **2014**, *299*, 1003−1012.
(69) Bandara, N.; Wu, J. Randomly Oriented Strand Board Composites from Nanoengineered Protein-Based Wood Adhesive. *ACS Sustainable Chem. Eng.* **2018**, *6*, 457−466.
(70) Sarmin, S. N.; Zakaria, S. A. K. Y.; Kasim, J.; Shafie, A. Influence of Resin Content and Density on Thickness Swelling of Three-Layered Hybrid Particleboard Composed of Sawdust and Acacia Mangium. *BioResources* **2013**, *8*, 4864−4872.
(71) Griffini, G.; Passoni, V.; Suriano, R.; Levi, M.; Turri, S. Polyurethane Coatings Based on Chemically Unmodified Fractionated Lignin. *ACS Sustainable Chem. Eng.* **2015**, *3*, 1145−1154.
(72) Zhu, X.; Wang, D.; Li, N.; Sun, X. S. Bio-Based Wood Adhesive from Camelina Protein (a Biodiesel Residue) and Depolymerized Lignin with Improved Water Resistance. *ACS Omega* **2017**, *2*, 7996−8004.
(73) Zheng, P.; Chen, N.; Mahfuzul Islam, S. M.; Ju, L. K.; Liu, J.; Zhou, J.; Chen, L.; Zeng, H.; Lin, Q. Development of Self-Cross-Linked Soy Adhesive by Enzyme Complex from Aspergillus Niger for Production of All-Biomass Composite Materials. *ACS Sustainable Chem. Eng.* **2019**, *7*, 3909−3916.
(74) Hemmilä, V.; Adamopoulos, S.; Karlsson, O.; Kumar, A. Development of Sustainable Bio-Adhesives for Engineered Wood Panels-A Review. *RSC Adv.* **2017**, *7*, 38604−38630.

https://doi.org/10.1021/acssuschemeng.1c01916
ACS Sustainable Chem. Eng. 2021, 9, 10990−11002